Received: 18 December 2025 | Revised: 2 February 2026 | Accepted: 24 February 2026 | Published online: 9 March 2026

RESEARCH ARTICLE

Medinformatics
2026, Vol. 00(00) 1–14
DOI: 10.47852/bonviewMEDIN62028824

BON VIEW PUBLISHING

Integrative Network Pharmacology and Docking Analysis of *Moringa oleifera* in Alzheimer's Disease: Dual Targeting of MAPK1 and STAT3 by Active Phytochemical Compounds

Israr Hussain[1, †], Itazaz Ul Haq[2, †], Muhammad Rahiyab[1], Li Pinyi[2], Ishaq Khan[1], Syed Shujait Ali[1], Mohammad Ali[1] and Arshad Iqbal[1,*]

[1] *Centre for Biotechnology and Microbiology, University of Swat, Pakistan*

[2] *College of Life Science, Sichuan Agricultural University, China*

Abstract: Alzheimer's disease (AD) is a multifactorial neurodegenerative disorder with limited therapeutic options. This study evaluated the potential of *Moringa oleifera* as a multi-target therapeutic candidate for AD using an integrative network pharmacology and molecular docking approach. From 209 screened phytochemicals, six compounds—hesperetin, cianidanol, campesterol, 24-methylenecholesterol, β-sitosterol, and 28-isoavenasterol acetate—met drug-likeness and oral bioavailability criteria. Target prediction identified 233 overlapping genes between *M. oleifera* compounds and AD-associated genes, forming a densely interconnected protein–protein interaction network with key hub proteins including HSP90AA1, SRC, MAPK1, and STAT3. Functional enrichment analysis revealed significant involvement in MAPK signaling, neuroactive ligand–receptor interaction, arachidonic acid metabolism, and amyloid-beta response pathways. Molecular docking demonstrated that sterol derivatives, particularly campesterol and 24-methylenecholesterol, exhibited the strongest binding affinities to MAPK1 (−8.2 kcal/mol), stabilizing critical residues such as ALA52, ILE31, VAL39, ASP111, and ASP167. In contrast, flavonoids such as hesperetin and cianidanol showed moderate binding affinities but more favorable pharmacokinetic and safety profiles. Several compounds also interacted with STAT3 at moderate affinities, suggesting partial modulation of neuroinflammatory signaling. Overall, these findings suggest that *M. oleifera* may exert neuroprotective effects through dual targeting of MAPK1-driven neuronal dysfunction and STAT3-mediated inflammation. These results are based on computational analyses and should be considered hypothesis-generating, warranting further experimental validation.

Keywords: *M. oleifera*, Alzheimer's disease, MAPK1 inhibition, STAT3 signaling, network pharmacology

1. Introduction

Alzheimer's disease (AD) constitutes the primary cause of dementia, representing a progressive neurodegenerative disorder with escalating global prevalence. Its pathogenesis is characterized by the accumulation of extracellular amyloid-beta (Aβ) plaques, intracellular neurofibrillary tangles of hyperphosphorylated tau protein, chronic neuroinflammation, and extensive synaptic and neuronal loss [1]. The therapeutic landscape for AD remains highly limited. Monotherapeutic strategies, including recent anti-Aβ immunotherapies, have demonstrated only marginal clinical efficacy, frequently accompanied by significant adverse effects [2]. These persistent failures underscore the insufficiency of the single-target paradigm and highlight the necessity for polypharmacological interventions that address the multifactorial nature of AD pathogenesis.

Medicinal plants with documented traditional use represent a viable source of multi-target therapeutic agents. *Moringa oleifera* is widely employed in traditional medicinal systems and has demonstrated a range of pharmacological activities, including antioxidant, anti-inflammatory, and neuroprotective effects [3]. Phytochemical investigations have identified numerous bioactive constituents, such as flavonoids (e.g., quercetin, kaempferol), glucosinolates (e.g., glucotropaeolin), and phenolic acids (e.g., chlorogenic acid) [4]. The specific molecular mechanisms through which *M. oleifera* modulates AD pathology remain poorly defined and have not been systematically investigated using a systems-level approach.

In comparison with other medicinal plants used in neurodegenerative research, such as *Ginkgo biloba* and *Withania somnifera*, *M. oleifera* possesses a uniquely diverse phytochemical profile enriched with sterols, flavonoids, glucosinolates, isothiocyanates, and phenolic acids. Compounds such as quercetin,

***Corresponding author:** Arshad Iqbal, Centre for Biotechnology and Microbiology, University of Swat, Pakistan. Email: arshad.iqbal@uswat.edu.pk
† **Co-first author**

kaempferol, β-sitosterol, and campesterol exhibit stronger antioxidant and anti-inflammatory activities relative to several bioactives isolated from *G. biloba* and *W. somnifera* [5]. *M. oleifera* contains rare sterol derivatives such as 24-methylenecholesterol and 28-isoavenasterol acetate, which have been increasingly recognized for their neuroprotective, anti-amyloidogenic, and MAPK-modulating properties [3]. These compounds provide a broader multi-target pharmacological spectrum, making *M. oleifera* particularly suitable for systems-level interventions in AD [6]. Given this phytochemical richness and its long-standing traditional use for cognitive enhancement, *M. oleifera* represents a promising candidate for integrative computational analysis and therapeutic exploration.

Conventional reductionist methodologies are inadequate for deciphering the complex interactions between a multi-constituent natural product and a multifaceted disease like AD. Network pharmacology, which integrates bioinformatics, systems biology, and polypharmacology, provides a powerful framework for the holistic prediction of drug-target-disease interactions and the elucidation of underlying therapeutic mechanisms [7]. This approach is particularly suited for validating the traditional applications of *M. oleifera* and for mapping its complex pharmacodynamics.

In this study, we applied an integrative network pharmacology approach to delineate the therapeutic potential of *M. oleifera* against AD. We systematically identified its bioactive compounds, predicted their high-confidence protein targets, and constructed a comprehensive interaction network with AD-associated genes. Topological analysis of the protein–protein interaction (PPI) network identified several critical hub targets, including HSP90AA1, MAPK1, and STAT3. Functional enrichment analysis revealed significant involvement in MAPK1 signaling and neuroactive ligand–receptor interaction pathways. Our analysis identified the MAPK1 signaling axis as a central and previously unreported mechanism for *M. oleifera* in the context of AD. This target nexus is strategically positioned at the intersection of neuroinflammation and synaptic regulation, core processes in AD that are not effectively addressed by current monotherapies.

Advancements in computational drug discovery have significantly accelerated the identification of therapeutic candidates for neurodegenerative diseases, particularly AD. AI-assisted target prediction tools, such as deep learning–based chemo genomic models and AlphaFold2-derived structural data, have greatly improved the accuracy of protein–ligand interaction predictions [8]. Multi-omics integrated network pharmacology frameworks now allow the reconstruction of disease-specific molecular networks, enabling the identification of high-value targets such as MAPK1 and STAT3 that sit at the intersection of inflammation, synaptic dysfunction, and neuronal survival [9]. Modern docking approaches utilizing deep learning scoring functions and enhanced sampling techniques have increased the reliability of virtual screening pipelines. These computational advances have provided a strong foundation for combining network pharmacology, docking, and molecular dynamics (MD) to explore the multi-target therapeutic potential of natural products, including *M. oleifera*, in AD [10].

This study provides a systematic, molecular-level foundation for the traditional use of *M. oleifera* in cognitive disorders. It delineates a multi-target mechanism of action and identifies novel, high-value target pathways, thereby offering a compelling rationale for subsequent experimental validation and positioning *M. oleifera* as a promising source for multi-target therapeutic strategies or nutraceutical interventions in AD. The overall workflow of the entire study is described in Figure 1.

2. Materials and Methods

2.1. Data collection and active compounds screening in *Moringa oleifera*

Data on the active compounds of *M. oleifera* were obtained through a review of existing literature and publicly accessible databases. Specifically, information on compounds associated with *M. oleifera* was compiled from phytochemical databases such as IMPPAT (https://cb.imsc.res.in/imppat/) [11] and KNApSAcK-3D Phytochemical and Ethnobotanical Database (http://www.knapsackfamily.com/KNApSAcK/) [12]. A comprehensive literature search was conducted using PubMed (https://pubmed.ncbi.nlm.nih.gov/) [13] and Google Scholar (https://scholar.google.com/) [14] with the primary keyword "*M. oleifera*." Relevant research articles and compound data were retrieved using the term "*M. oleifera*." Screening of these compounds was performed to identify promising drug-like molecules. The selection criteria were oral bioavailability (OB) score > 50%, a drug-likeness (DL) score > 0.50, and a molecular weight (MW) < 500 g/mol. OB, MW, and DL scores were computationally predicted using SwissADME (http://www.swissadme.ch/) [15] and Molsoft (https://www.molsoft.com/mprop/) [16]. Compound structures, canonical SMILES, and molecular data were retrieved from the PubChem (https://pubchem.ncbi.nlm.nih.gov/) [17] and ChemSpider (http://www.chemspider.com/) [18] databases.

2.2. Target identification and network construction

Target prediction serves as the foundational step for mapping molecular interactions between phytochemicals and disease pathways. The putative protein targets of bioactive compounds were identified using their Simplified Molecular-Input Line-Entry System (SMILES) notations. These notations were submitted to the Swiss Target Prediction (http://www.swisstargetprediction.ch/) [19], which forecasts human protein targets based on structural similarity and known interactions. Only targets meeting a high-confidence threshold (probability ≥ 0.5 for Swiss Target Prediction) were retained.

AD-related genes were compiled from the GeneCards (https://www.genecards.org/) [20] and OMIM databases (https://www.omim.org/) [21] to establish a comprehensive disease gene set. Common gene symbols were resolved using UniProtKB (https://www.uniprot.org/) [22], and overlap between phytochemical compound targets and AD genes was determined and visualized using Venny 2.1 (https://bioinfogp.cnb.csic.es/tools/venny/) [23] to identify common genes for network construction.

2.3. PPI network construction and hub gene identification

To investigate the system-level mechanisms underlying the potential therapeutic effects of *M. oleifera* in AD, a PPI network was generated using the 233 common genes identified through target prediction analysis. The PPI data were obtained from the STRING database version 11.5 (https://string-db.org/) [24], restricted to *Homo sapiens* as the target organism. A confidence threshold of combined score > 0.4 was applied to ensure inclusion of both high-confidence interactions and broader network connectivity. A medium-confidence interaction score (combined score > 0.4) was selected to balance interaction reliability with network coverage, allowing inclusion of both experimentally validated and high-confidence predicted protein interactions, which

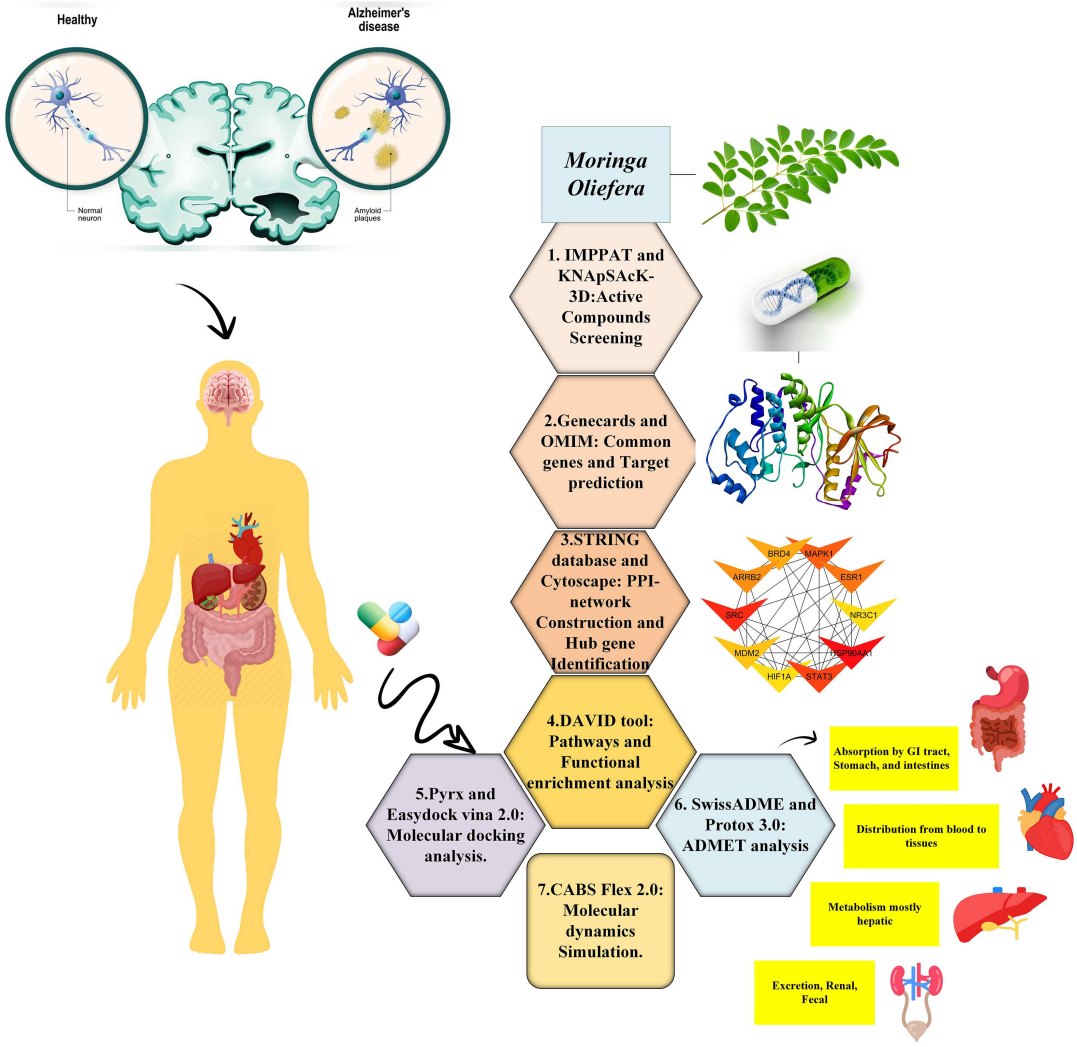

Figure 1. Computational workflow for investigating the neuroprotective potential of *M. oleifera* against Alzheimer's disease

is appropriate for exploratory network pharmacology analyses aimed at identifying hub targets.

The resulting interaction network was imported into Cytoscape software (version 3.9.1) in TSV format for visualization and computational analysis [25]. Network topology was examined using established graph theoretical parameters, with particular emphasis on degree centrality as a primary metric for identifying hub genes. Nodes exhibiting the highest degree values were designated as network hubs, representing proteins of potential biological significance in the mechanism of action of *M. oleifera* compounds against AD pathology. These hub genes were prioritized for subsequent functional enrichment analyses to elucidate their roles in relevant biological pathways and processes.

2.4. Pathways and functional enrichment analysis

Functional enrichment analysis was conducted to systematically characterize the biological roles and pathways associated with the 233 common target genes. Gene ontology (GO) annotation and Kyoto Encyclopedia of Genes and Genomes (KEGG) pathway enrichment were performed using the DAVID bioinformatics resource (version 6.8) [26]. This analysis categorized gene functions into three primary domains: biological process (BP), molecular function (MF), and cellular component (CC). All GO and KEGG enrichment analyses were performed using the entire human genome (*Homo sapiens*) as the background reference set, as implemented in both DAVID 6.8 and STRING 11.5. The STRING database was additionally employed to corroborate the functional enrichment findings through its integrated protein association networks. Statistically significant terms were identified using a threshold of $p < 0.05$, adjusted for multiple testing using the Benjamini–Hochberg false discovery rate (FDR) correction. Enrichment results were visualized using bubble plots generated through the SR Plot platform (https://www.bioinformatics.com.cn/srplot) [27], which provided a quantitative representation of enrichment significance ($-\log10(p\text{-value})$) and gene count ratios for each term.

Multiple testing correction was uniformly applied using the Benjamini–HochbergFDR, and only terms with adjusted p-values < 0.05 were considered statistically significant.

The most significantly enriched GO terms and KEGG pathways were selected for further biological interpretation based on statistical rigor and relevance to AD pathogenesis.

2.5. Molecular docking analysis

A molecular docking study was conducted to evaluate the binding interactions and affinities of the compounds against

selected protein targets. This approach is a pivotal tool in structure-based drug design for predicting the preferred orientation and binding energy of a small-molecule ligand within a protein's active site. The three-dimensional crystal structures of the target proteins STAT3 PDB ID:6D5Y and MAPK1 PDB ID: 6NJS were retrieved from the RCSB Protein Data Bank (https://www.rcsb.org/) [28]. The protein structures were prepared using PyMOL [29]. This preparation involved the removal of water molecules, co-crystallized ligands, and any heteroatoms not pertinent to the binding site. Polar hydrogen atoms were added, and the structures were energy-minimized to correct any steric clashes. PyRx software (version 0.8) was utilized for the energy minimization of these ligands and for converting them into the PDBQT format, which is required for docking calculations [30]. For MAPK1, the grid box was defined using EasyDock Vina with dimensions centered on the active-site coordinates obtained from the co-crystallized ligand binding pocket. The Auto Grid dimensions were set as follows: grid center coordinates X = 6.6131, Y = 9.2389, Z = 22.5476 and number of points X = 81, Y = 58, Z = 70, defining the spatial grid settings for a molecular modeling or docking simulation using a protein data file. The box was large enough to cover the entire catalytic site and adjacent regulatory regions. The actual docking simulations were performed using EasyDock Vina (v. 2.2) [31]. For each ligand–protein complex, multiple binding poses were generated. Each ligand was docked using an exhaustiveness value of 8, and 10 independent docking runs were performed per compound to ensure sampling consistency and convergence toward the lowest-energy binding pose. The best docking pose for each ligand was selected based on the lowest binding affinity (ΔG, kcal/mol) combined with inspection of key interactions (hydrogen bonds, hydrophobic contacts, and orientation within the active site). Poses with steric clashes or inconsistent orientations were excluded.

The primary criteria for evaluating the docking results were:

1. The binding affinity (ΔG), expressed in kcal/mol, with more negative values indicating stronger binding.
2. The root mean square deviation (RMSD) of the atomic positions for the top-ranked poses, used to assess the reliability and consistency of the docking run.

The resulting docked complexes for the most favorable poses (lowest binding energy) were visualized and analyzed using Discovery Studio Visualizer to identify and depict key molecular interactions [32].

2.6. ADMET profiling and pharmacokinetic evaluation

ADMET (Absorption, Distribution, Metabolism, Excretion, and Toxicity) properties are critical determinants of a compound's viability as a drug candidate. Early-stage ADMET profiling helps identify potential pharmacokinetic and safety issues, reducing late-stage attrition in drug development. In this study, we employed computational tools to evaluate key ADMET parameters for the designed compounds, ensuring a balance between efficacy and safety. The SwissADME tool (http://www.swissadme.ch) was used to compute physicochemical descriptors (e.g., molecular weight, lipophilicity, hydrogen bonding) and assess DL based on guidelines like Lipinski's Rule of Five [33]. The Bioavailability Radar provided a visual overview of compound suitability for oral administration. ProTox-3.0 (https://tox.charite.de/protox3/index.php?site=home) predicted organ toxicity (e.g., hepatotoxicity), toxicological endpoints (e.g., mutagenicity, carcinogenicity), and toxicity targets using machine learning models and molecular similarity [34].

2.7. Molecular dynamics simulation

To validate the dynamic stability of the compound–protein interactions obtained from molecular docking, MD simulations were performed using the CABS-flex 2.0 server (https://biocomp.chem.uw.edu.pl/CABSflex2/submit) [35]. This platform employs a coarse-grained protein model to simulate protein flexibility and ligand interactions while maintaining computational efficiency. The top six phytochemicals identified from docking analysis—campesterol, 24-methylenecholesterol, β-sitosterol, 28-isoavenasterol acetate, hesperetin, and cianidanol—were selected for MD evaluation against the MAPK1 protein.

Each protein–ligand complex was subjected to a 10 ns simulation run with default parameters. Residue-level fluctuations were analyzed in terms of root mean square fluctuation (RMSF, Å) values, which represent the average displacement of each residue over time relative to its mean position. Lower RMSF values indicate greater structural stability, whereas higher fluctuations suggest localized flexibility. RMSF profiles were extracted from the simulation output, and descriptive statistics (mean, standard deviation, minimum, maximum) were calculated for each complex [36]. As this is an in silico study, the computational predictions require future validation through in vitro MAPK1 activity assays, STAT3 inhibition assays, and neuroinflammatory marker evaluation.

3. Results

3.1. Screening of bioactive compounds from *M. oleifera*

A comprehensive phytochemical library of *M. oleifera* was constructed by aggregating data from two specialized databases: the IMPPAT database contributed 201 compounds, and the KnapSack server contributed 77 compounds, yielding an initial total of 278 bioactive phytochemical compounds. This raw compound collection underwent a curation process to eliminate redundancies. Manual inspection and removal of duplicate entries in Microsoft Excel resulted in a refined, non-redundant library of 209 unique phytochemical compounds for subsequent pharmacokinetic evaluation. This refined library was then subjected to the predefined virtual screening filters based on the criteria of oral bioavailability (OB > 50%), drug-likeness (DL > 0.50), and molecular weight (MW < 500 g/mol). The application of these ADMET parameters predicted six compounds that met all criteria and were selected for further computational investigation. These findings are predictive in nature and highlight computationally derived interactions that require validation through biochemical and cellular experiments. The names and key properties of these screened compounds are presented in Supply Table 1.

3.2. Identification of AD-related targets

The six active compounds identified from *M. oleifera* were submitted to the SwissTarget Prediction database, yielding a total of 256 target genes. 15,563 genes associated with AD were compiled from the GeneCards and OMIM databases.

Venn diagram analysis identified an overlap of 226 common genes between the *M. oleifera*-derived compound targets and

Table 1. Molecular docking results and binding interactions of the active compounds with MAPK1

Compound	Binding affinity (kcal/mol)	PubChem ID	Target protein	Category
Campesterol	–8.2	173183	MAPK1	Active compound in *M. oleifera*
24-Methylenecholesterol	–8.2	92113	MAPK1	Active compound in *M. oleifera*
Beta-sitosterol	–8.0	222284	MAPK1	Active compound in *M. oleifera*
NJK14047	–8.0	135395450	MAPK1	REFRENCE INHIBITOR
Neflamapimod VX-745	–7.6	3038525	MAPK1	REFRENCE INHIBITOR
28-Isoavenasterol acetate	–7.3	91746804	MAPK1	Active compound in *M. oleifera*
Hesperetin	–6.9	72281	MAPK1	Active compound in *M. oleifera*
Cianidanol	–6.8	9064	MAPK1	Active compound in *M. oleifera*
28-Isoavenasterol acetate	–6.2	91746804	STAT3	Active compound in *M. oleifera*
24-Methylenecholesterol	–5.9	92113	STAT3	Active compound in *M. oleifera*

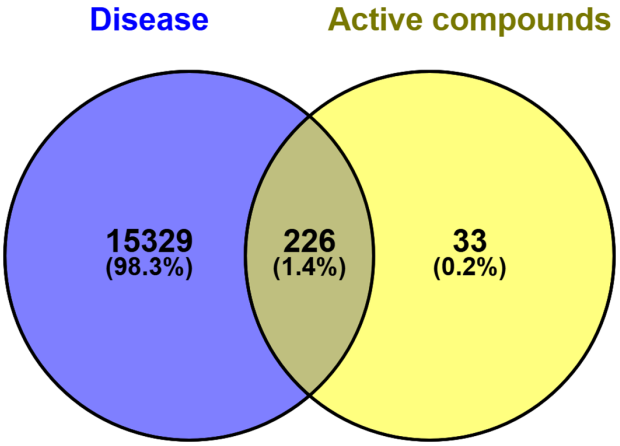

Figure 2. Venn diagram showing the overlap between *M. oleifera* compound targets and Alzheimer's disease-associated genes (226 common targets)

AD-related genes (Figure 2). These overlapping genes were considered computationally predicted candidate targets and were selected for subsequent network and pathway analysis to explore potential interactions.

3.3. Network pharmacology analysis

The 233 common genes, considered computationally predicted therapeutic targets of *M. oleifera* against AD, were submitted to the STRING database (version 11.5) to construct a PPI network. The network was generated with a high-confidence interaction score threshold of > 0.4. The resulting network data was downloaded in TSV format and imported into Cytoscape software (version 3.9.1) for further visualization and topological analysis.

The resulting network comprised 226 nodes and 2099 edges (Figure 3). The high average node degree of 18.6 and an average local clustering coefficient of 0.476 indicate a densely interconnected and modular network structure. The PPI enrichment *p*-value of < 1.0e-16 indicates that the observed number of interactions is greater than expected by chance for a random set of proteins of similar size, suggesting a potentially coherent network structure. This suggests that the computationally predicted targets of *M. oleifera* bioactive form a closely linked network in silico. The top 10 proteins ranked by degree centrality are listed in Supply Table 2. HSP90AA1 and SRC showed the highest connectivity, with degree scores of 57 and 53, indicating their predicted role as hub proteins within the network. The top 10 proteins ranked by maximal clique centrality (MCC) are listed in Supply Table 3. AR showed the highest MCC score, indicating its predicted involvement in the largest number of fully connected subnetworks (Figure 4a and b).

3.4. Functional enrichment gene ontology analysis

Functional enrichment analysis identified computationally predicted potentially biological processes associated with *M. oleifera* compounds and AD-related genes. KEGG pathway analysis showed significant enrichment in neuroactive ligand–receptor interaction and arachidonic acid metabolism, suggesting potential involvement in neurotransmission- and neuroinflammation-related pathways.

GO analysis demonstrated enrichment in key biological processes including response to amyloid-beta and positive regulation of cytosolic calcium ion concentration, highlighting computationally predicted associations with AD-related pathways. MFs were dominated by protein kinase activity and transition metal ion binding, potentially related to cell signaling and metal ion homeostasis. CC localization highlighted synaptic membrane and presynaptic membrane associations, suggesting that these proteins may be localized to neuronal structures relevant in AD. The most significant GO terms and pathways, ranked by p-value and gene count, are presented graphically in Figure 5, which categorizes the findings into (5a) MF, (5b) CC, (5c), KEGG pathway, and (5d) BP.

The convergence of these enriched terms indicates that *M. oleifera* compounds are computationally predicted to be involved in pathways related to synaptic function, inflammatory response, and cellular homeostasis relevant to AD.

In Supply Figure 1a, a chord plot illustrates the associations between hub genes (red nodes) and enriched biological processes, including calcium ion homeostasis, amyloid-beta response, MAPK signaling regulation, and steroid metabolism. The bar chart in Supply Figure 1b presents the GO enrichment results across the three main ontologies: BP, CC, and MF. The most significantly enriched biological processes included steroid metabolic process, regulation of cytosolic calcium ion concentration, positive regulation of the MAPK cascade, and response to amyloid-beta.

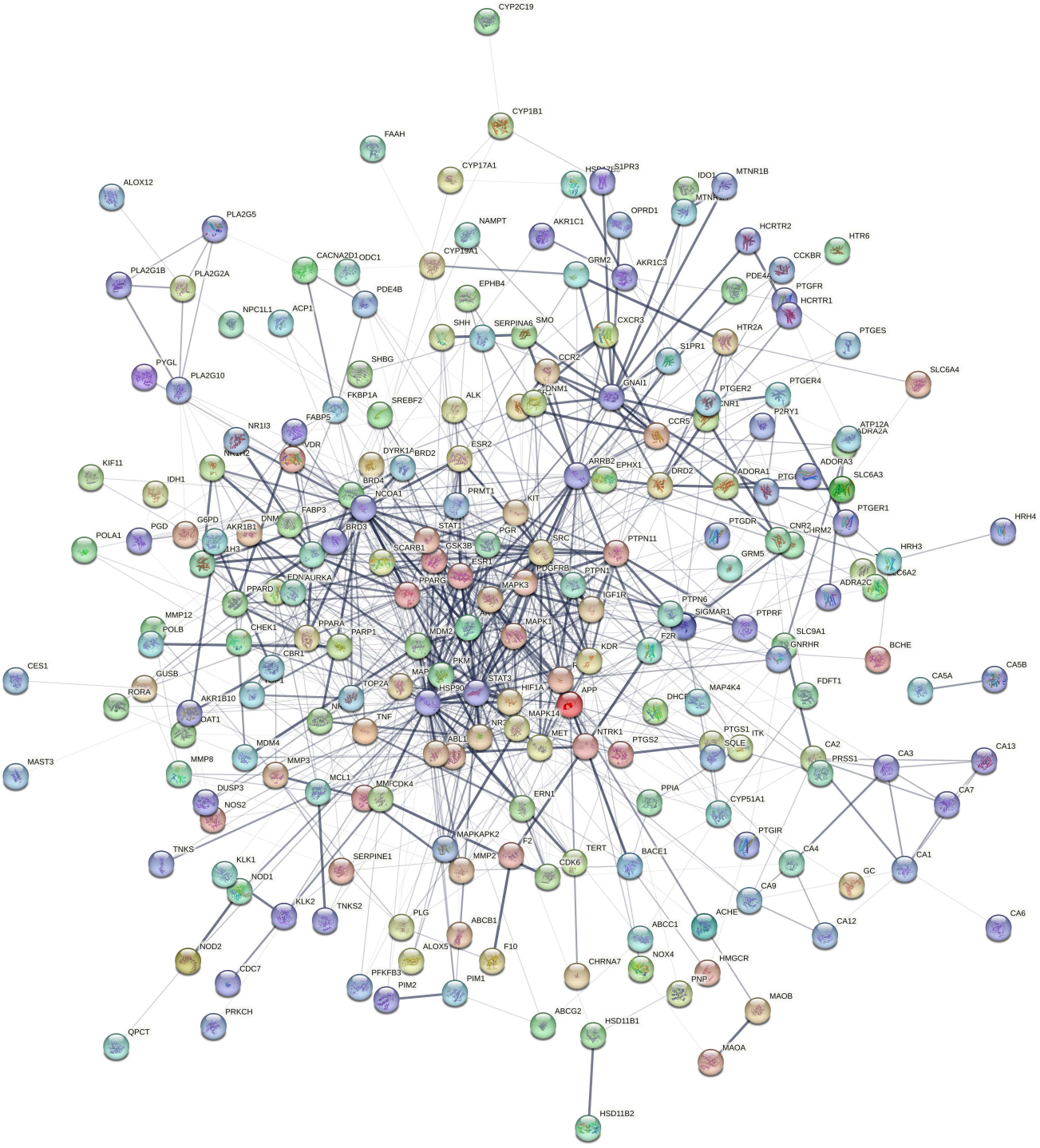

Figure 3. Protein–protein interaction (PPI) network of 233 overlapping genes. Nodes represent proteins, and edges represent interactions

3.5. Molecular docking results section

The three-dimensional (3D) structures of MAPK1 and STAT3 were retrieved and analyzed. Supply Figure 2a shows the 3D structure of the MAPK1 protein, and Supply Figure 2b presents the 3D structure of STAT3. The molecular docking analysis was performed to evaluate the binding affinity and interaction patterns of the six bioactive compounds from *M. oleifera* against the MAPK1 (ERK2) and STAT3 protein targets. The results demonstrated that all compounds exhibited comparatively higher predicted binding affinity toward the MAPK1 protein compared to the STAT3 protein. Specifically, campesterol and 24-methylenecholesterol showed the lowest predicted binding energies toward MAPK1, with binding energies of −8.2 kcal/mol each, suggesting them as the most promising candidates for further investigation (Supply Figures 3 and 4).

The binding affinities (ΔG in kcal/mol) for all compounds against MAPK1 are summarized in Table 1. The binding energies ranged from −6.8 to −8.2 kcal/mol. Campesterol and 24-methylenecholesterol displayed the lowest predicted binding

Table 2. Molecular interaction profiles of active compounds in *M. oleifera* with MAPK1

Compound	Hydrogen bonds (residues)	Other significant interactions
Cianidanol	5 (ASP111, GLN106, ASP167, SER153, ASN155)	Pi-sigma LEU156, Alkyl (ALA52) Van der Waals interactions
Hesperetin	4 (ASN154, ASP167, LYS54, GLN106)	Pi-sigma LEU156 Pi-alkyl ALA52 Pi-anion ASP 111 Van der Waals
24-Methylenecholesterol	2 (GLU109, MET108)	Alkyl (ALA52, VAL39, ILE31) Van der Waals (GLU33, GLY34, LYS54)
28-Isoavenasterol acetate	1 (GLU109)	Alkyl (ALA35,52,189, ILE31) Van der Walls (ASP149,167,169)
Beta-sitosterol	No hydrogen bond interaction	Alkyl (LEU107,156, ILE31, VAL39, LYS54) Van der Waals (ASP111,167, THR110)
Campesterol	No hydrogen bond interaction	Alkyl (ALA35,52, ILE31, VAL39) Van der Waals (GLU33, GLY34, LYS54, ASP111,167,169,154)

Table 3. Predicted ADMET properties of bioactive compounds from *M. oleifera*

Property	Hesperetin	Cianidanol	24-Methylenech olesterol	28-Isoavenasterol acetate	Campesterol	Beta-sitosterol
PubChem CID	72281	9064	92113	91746804	173183	222284
iLOGP	2.24	1.33	4.83	4.96	4.97	5.05
GI Absorption	High	High	Low	Low	Low	Low
BBB Permeant	No	No	No	No	No	No
P-gp Substrate	Yes	Yes	No	No	No	No
CYP1A2 Inhibitor	Yes	No	No	No	No	No
CYP2C9 Inhibitor	No	No	Yes	No	No	No
CYP3A4 Inhibitor	Yes	No	No	No	No	No
Lipinski Violations	0	0	1	1	1	1

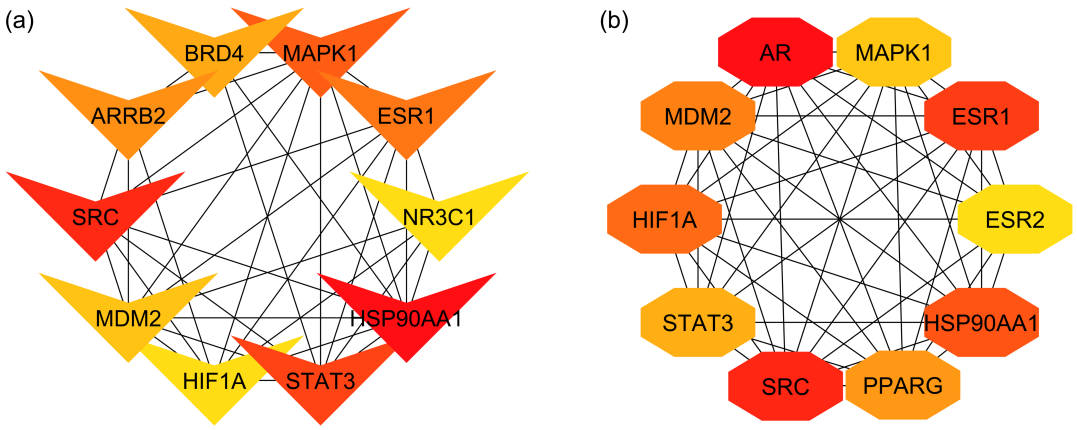

Figure 4. (a) Top 10 protein interactions ranked by degree method; (b) Top 10 protein interactions ranked by MCC method

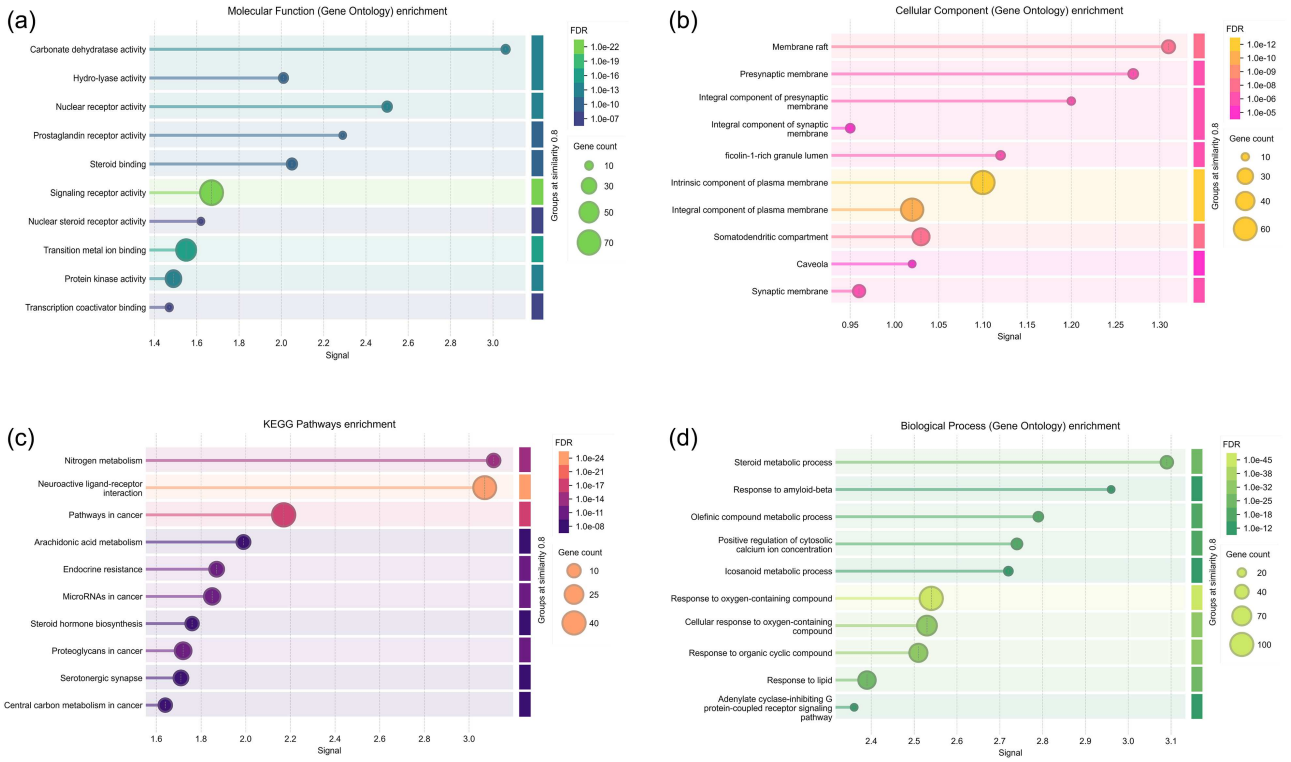

Figure 5. GO enrichment analysis results of overlapping target genes categorized into (a) molecular function, (b) cellular component terms, (c) KEGG pathway, and (d) biological process

energies among the tested compounds, slightly lower than the reference inhibitors (NJK14047: −8.0 kcal/mol; neflamapimod: −7.6 kcal/mol) [37, 38]. The consistently strong binding affinities of these natural compounds suggest favorable computational interactions with MAPK1. The docking results with STAT3 revealed significantly weaker binding affinities for all compounds. 28-Isoavenasterol acetate and 24-methylenecholesterol showed the highest binding energies among the compounds against STAT3, with values of −6.2 and −5.9 kcal/mol, respectively, which are relatively lower than their predicted binding to MAPK1. This difference in predicted binding energies indicates a preferential computational interaction of these compounds with MAPK1 compared to STAT3.

The molecular interaction profiles between active compounds from *M. oleifera* and the MAPK1 protein were analyzed to assess binding affinities and interaction types. As shown in Table 2, cianidanol exhibited the highest number of hydrogen bonds (five), interacting with key residues such as ASP111, GLN106, and ASP167, along with additional Pi-sigma and alkyl interactions. Hesperetin formed four hydrogen bonds and demonstrated π-π and π-anion interactions with residues like LEU156 and ASP111. 24-Methylenecholesterol and 28-isoavenasterol acetate formed fewer hydrogen bonds but displayed notable hydrophobic (alkyl) and van der Waals interactions. Beta-sitosterol and campesterol did not form hydrogen bonds but engaged in several hydrophobic and van der Waals contacts with residues like ALA52, ILE31, and ASP111. These interactions suggest a range of binding mechanisms, with both polar and non-polar interactions contributing to the potential binding affinity of *M. oleifera* compounds toward MAPK1. All findings presented here reflect computational predictions and do not confirm biological activity; therefore, the proposed MAPK1/STAT3 modulation requires experimental validation.

3.6. ADMET profiling of active compounds and drug-likeness evaluation

Computational assessment of the six bioactive compounds from *M. oleifera* was conducted to evaluate key ADMET properties. Results, compiled in Tables 3 and 4, reveal distinct pharmacokinetic and toxicological profiles among the compounds.

Hesperetin and cianidanol were predicted to have high gastrointestinal absorption, suggesting potential oral bioavailability in silico. In contrast, the sterol-derived compounds 24-methylenecholesterol, 28-isoavenasterol acetate, campesterol, and β-sitosterol exhibited low absorption potential, likely attributable to elevated lipophilicity (iLOGP > 4.8) and molecular bulk. None of the analyzed compounds were predicted to permeate the blood-brain barrier, minimizing concerns related to central nervous system exposure. Metabolic profiling indicated notable cytochrome P450 (CYP) inhibition potential. Hesperetin was predicted to inhibit CYP1A2 and CYP3A4, suggesting a possible risk for pharmacokinetic drug–drug interactions. Additionally, 24-methylenecholesterol showed inhibitory activity against CYP2C9. The remaining compounds exhibited no significant inhibition of major CYP isoforms. DL evaluation via Lipinski's Rule of Five revealed zero violations for hesperetin and cianidanol, whereas all sterol compounds incurred one violation, primarily due to high octanol-water partition coefficients or molecular weight.

Toxicological assessment highlighted several critical safety concerns. Immunotoxicity was predicted to be of high risk for all sterol compounds, with hesperetin presenting a moderate risk. Cardiotoxicity was flagged for hesperetin with high confidence, potentially correlated to its CYP inhibitory activity. Furthermore, 28-isoavenasterol acetate indicated a medium risk level for both carcinogenicity and hormone receptor disruption, implying

Table 4. Toxicity profile prediction for six compounds based on ProTox-3.0 analysis. Risk levels are assigned based on prediction probability and clinical severity: High Risk (●) for high-probability high-severity endpoints (e.g., Immunotoxicity @ 0.99), Medium Risk (○) for moderate probability or lower severity endpoints, and Low/No Risk (◌) for inactive predictions or very low probability alerts.

Toxicity endpoint	24-Methylenecholesterol	28-Isoavenasterol acetate	Campesterol
Immunotoxicity	● High Risk	● High Risk	● High Risk
Cardiotoxicity	◌ Low/No Risk	○ Medium Risk	◌ Low/No Risk
Neurotoxicity	○ Medium Risk	◌ Low/No Risk	○ Medium Risk
Nephrotoxicity	◌ Low/No Risk	◌ Low/No Risk	◌ Low/No Risk
Respiratory Tox.	○ Medium Risk	○ Medium Risk	○ Medium Risk
Carcinogenicity	◌ Low/No Risk	○ Medium Risk	◌ Low/No Risk
Hormone Receptor	● High Risk	◌ Low/No Risk	◌ Low/No Risk
Toxicity Endpoint	**Beta-sitosterol**	**Hesperetin**	**Cianidanol**
Immunotoxicity	● High Risk	○ Medium Risk	◌ Low/No Risk
Cardiotoxicity	◌ Low/No Risk	● High Risk	◌ Low/No Risk
Neurotoxicity	○ Medium Risk	◌ Low/No Risk	◌ Low/No Risk
Nephrotoxicity	◌ Low/No Risk	○ Medium Risk	○ Medium Risk
Respiratory Tox.	○ Medium Risk	○ Medium Risk	○ Medium Risk
Carcinogenicity	◌ Low/No Risk	◌ Low/No Risk	◌ Low/No Risk
Hormone Receptor	◌ Low/No Risk	○ Medium Risk	◌ Low/No Risk

potential endocrine-modulating effects. Neurotoxic risk was moderate for 24-methylenecholesterol, campesterol, and β-sitosterol, while nephrotoxicity and respiratory toxicity profiles were generally low to moderate across the compound set. Hesperetin and cianidanol were predicted to have comparatively favorable pharmacokinetic profiles, although their predicted toxicity risks, particularly cardiotoxicity and immunotoxicity, require further experimental validation. The sterol compounds were predicted to have limited oral bioavailability and notable immunotoxic potential, which may limit their potential applicability. These computational insights provide a critical foundation for subsequent in vitro and in vivo toxicity studies and lead optimization efforts.

3.7. MD simulation and RMSF analysis

The RMSF analysis of MAPK1 in complex with the top six *M. oleifera* compounds is summarized in Table 5. All six complexes demonstrated overall stability, with mean RMSF values ranging between 0.84 and 1.12 Å, indicating limited structural fluctuations during simulation. Among them, 28-isoavenasterol acetate showed the lowest mean RMSF (0.84 Å), suggesting the highest stability of binding, while 24-methylenecholesterol exhibited the highest mean RMSF (1.12 Å). Notably, localized high fluctuations (> 5 Å) were observed for campesterol and cianidanol, reflecting flexible loop regions of MAPK1 that may accommodate ligand binding without destabilizing the global structure.

The results are shown in Figure 6, where each panel represents MAPK1 complexed with a different ligand. In Figure 6A, campesterol induced stable fluctuations with localized peaks around loop regions, showing a maximum RMSF of approximately 5.4 Å. Figure 6B shows that 24-methylenecholesterol also demonstrated moderate flexibility (max RMSF ~4.8 Å), while maintaining stability in the protein's core. Figure 6C indicates that hesperetin maintained consistent stability across residues (max RMSF ~4.8 Å), correlating with its strong hydrogen bonding interactions.

In Figure 6D, cianidanol exhibited slightly higher fluctuations (max RMSF ~5.0 Å) but retained stable binding across most residues. Figure 6E reveals that β-sitosterol induced stable dynamics (max RMSF ~4.6 Å), with fluctuations mainly confined to loop regions. Figure 6F shows that 28-isoavenasterol acetate produced the lowest overall flexibility (mean RMSF = 0.84 Å, max ~3.2 Å), indicating the most stable complex formation among all tested ligands.

4. Discussion

This study employed an integrative network pharmacology and molecular docking strategy to unravel the therapeutic potential of *M. oleifera* bioactive compounds in AD. The results strongly support the hypothesis that *M. oleifera* may act via multi-target and multi-pathway regulation, offering advantages over single-target therapies, which have shown limited clinical efficacy in AD [39, 40]. Functional enrichment analyses revealed that *M. oleifera* compounds may act through multiple AD-relevant pathways. The MAPK signaling pathway emerged as particularly significant, given its central role in amyloid-β (Aβ)-induced neurotoxicity, tau phosphorylation, and neuronal apoptosis [41]. Enrichment in neuroactive ligand–receptor interactions highlights the potential modulation of synaptic signaling, while the arachidonic acid metabolism pathway underscores the regulation of neuroinflammation [42, 43].

Sterol-derived compounds such as campesterol and 24-methylenecholesterol displayed the strongest MAPK1 binding affinities (−8.2 kcal/mol), surpassing reference inhibitors (NJK14047: −8.0 kcal/mol; neflamapimod: −7.6 kcal/mol). Their interactions involved hydrophobic contacts with ALA52, ILE31,

Table 5. RMSF values (Å) of MAPK1 residues in complex with top compounds from CABS-flex 2.0 simulations

Compound	PubChem ID	Mean RMSF (Å)	Min RMSF (Å)	Max RMSF (Å)	Std. dev.
Campesterol	173183	1.11	0.13	5.41	0.84
24-Methylenecholesterol	92113	1.12	0.13	4.82	0.88
Hesperetin	72281	1.05	0.15	4.82	0.84
Cianidanol	9064	1.09	0.07	5.03	0.97
β-Sitosterol	222284	1.06	0.07	4.64	0.83
28-Isoavenasterol acetate	91746804	0.84	0.07	3.17	0.73

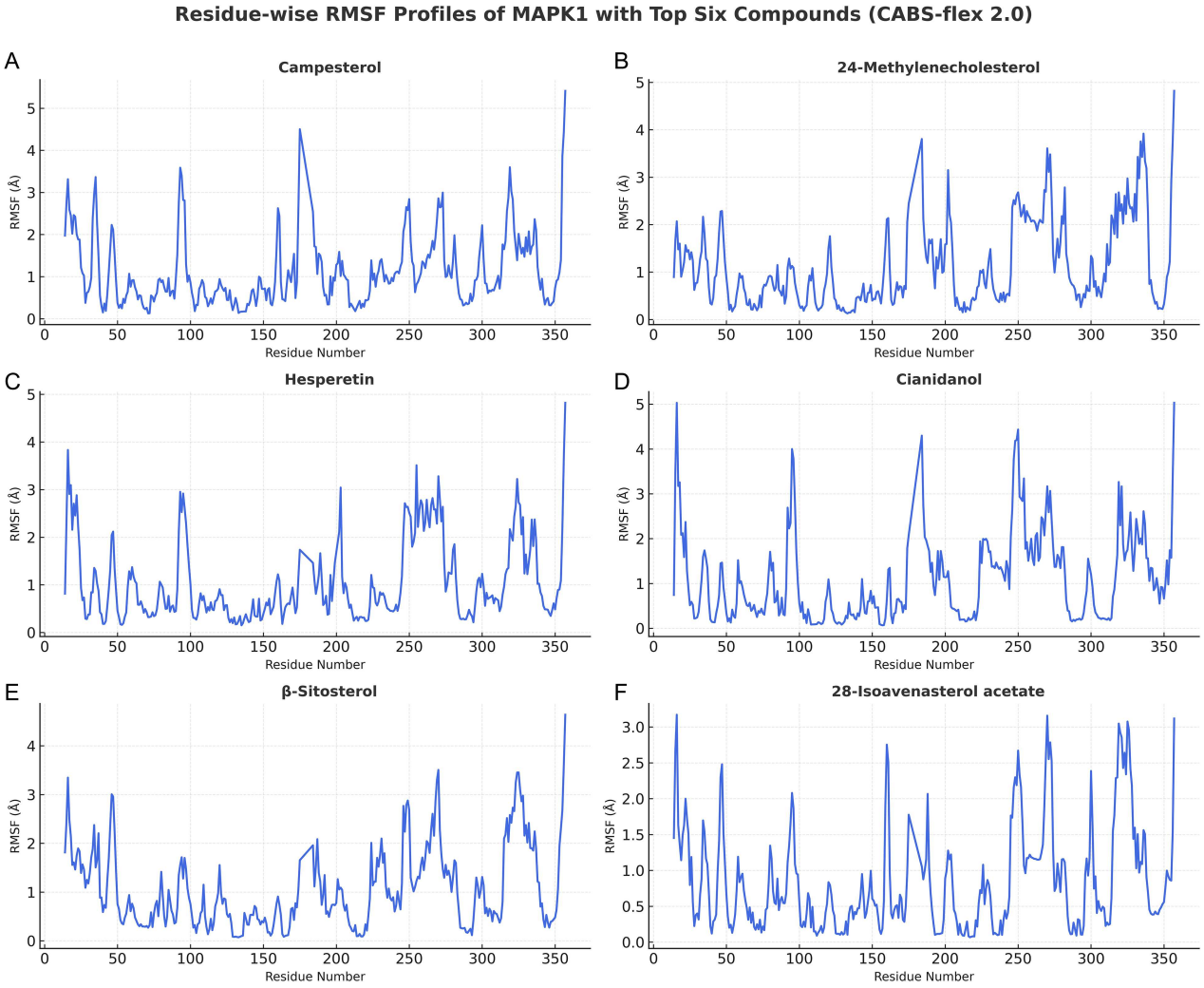

Figure 6. Residue-wise RMSF plot for MAPK1 bound with the six *M. oleifera* compounds. Residue-wise RMSF profiles of MAPK1 complexed with individual phytochemicals from *M. oleifera* using CABS-flex 2.0 simulations. (A) Campesterol, (B) 24-methylenecholesterol, (C) hesperetin, (D) cianidanol, (E) β-sitosterol, (F) 28-isoavenasterol acetate

and VAL39 and van der Waals stabilization with ASP111 and ASP167, indicating robust occupation of MAPK1's active pocket. Among the flavonoids, hesperetin and cianidanol exhibited weaker affinities (−6.9 and −6.8 kcal/mol, respectively) but formed multiple hydrogen bonds. Hesperetin bonded with ASN154, ASP167, LYS54, and GLN106, with an additional π-anion interaction at ASP111, while cianidanol formed five hydrogen bonds (ASP111, GLN106, ASP167, SER153, ASN155). Importantly, hesperetin and cianidanol also demonstrated favorable pharmacokinetics, including high gastrointestinal absorption and zero Lipinski violations, which highlight their suitability for oral delivery and nutraceutical development. 28-isoavenasterol acetate, while less potent against MAPK1 (−7.3 kcal/mol), showed unique dual-targeting ability by also binding STAT3 (−6.2 kcal/mol). This may position it as a multi-target regulator, though potential hormone receptor–disrupting effects warrant caution. MAPK1 (ERK2) is a crucial regulator of neuronal signaling, synaptic plasticity, and cell survival [44]. In AD, its overactivation has been linked to Aβ-induced synaptic dysfunction, tau hyperphosphorylation, and neuronal apoptosis. [45].

Our results indicate that *M. oleifera* sterol derivatives strongly interact with MAPK1, suggesting their potential to modulate or inhibit pathological MAPK1 activity. By stabilizing residues such as ASP111 and ASP167, these compounds may attenuate downstream tau phosphorylation and neuronal loss [46]. This finding aligns with prior evidence that MAPK inhibitors can reduce AD-related pathology, underscoring the therapeutic value of MAPK1 as a target.

STAT3, another identified hub protein, has a dual role in the central nervous system [47]. Under normal conditions, STAT3 supports neuronal survival and repair. However, in AD, aberrant STAT3 activation contributes to chronic neuroinflammation by sustaining microglial overactivation and promoting pro-inflammatory cytokine release. Persistent STAT3 signaling also disrupts mitochondrial bioenergetics, further impairing neuronal function. *M. oleifera* compounds, particularly 28-isoavenasterol acetate and 24-methylenecholesterol, bound STAT3 with moderate affinities (−6.2 and −5.9 kcal/mol, respectively). While weaker than MAPK1 interactions, these engagements suggest that *M. oleifera* may still modulate STAT3-driven neuroinflammation. Even partial suppression of STAT3 hyperactivity could alleviate glial-driven synaptic damage and inflammatory burden in AD brains. The convergence of MAPK1 and STAT3 as top targets underscores their complementary roles in AD: MAPK1 primarily drives Aβ- and tau-related neurotoxicity [48], while the ability of *M. oleifera* phytochemicals to interact with both proteins suggests a dual-target mechanism capable of simultaneously preserving neuronal integrity and suppressing chronic inflammation. This duality provides an important therapeutic advantage over existing monotherapies that often fail to address the complex, multifactorial nature of AD [49].

This study highlights *M. oleifera* as a rich source of multi-target compounds. Sterols such as campesterol and 24-methylenecholesterol demonstrate strong MAPK1 inhibition potential but require pharmacokinetic optimization due to poor absorption and immunotoxicity risk. Flavonoids such as hesperetin and cianidanol, with safer pharmacokinetic profiles, may be more suitable for direct therapeutic application. Together, these compounds provide a synergistic therapeutic strategy, targeting both neuronal degeneration and neuroinflammation through MAPK1 and STAT3 regulation.

The MD simulation results provide dynamic validation of the docking predictions, confirming that the binding of *M. oleifera* compounds to MAPK1 is generally stable under physiological-like conditions [8]. The relatively low mean RMSF values (< 1.2 Å for all complexes) indicate minimal perturbation of the MAPK1 backbone, supporting the hypothesis that these phytochemicals stabilize rather than disrupt protein structure [50]. Among the tested compounds, 28-isoavenasterol acetate demonstrated the lowest overall flexibility (mean RMSF = 0.84 Å), indicating the strongest stabilization effect on MAPK1. This is consistent with its moderate docking affinity (−7.3 kcal/mol) and suggests that despite lower binding energy compared to sterols like campesterol, its dynamic fit within the MAPK1 active pocket may provide functional relevance. Sterol compounds (campesterol, 24-methylenecholesterol, and β-sitosterol) showed slightly higher mean RMSF values (~1.1 Å), coupled with localized flexibility peaks (up to 5.4 Å for campesterol) [51]. These fluctuations are likely attributable to loop regions surrounding the active site, which remain mobile during ligand engagement. Such moderate flexibility is not inherently destabilizing and may facilitate induced-fit interactions that strengthen binding. Flavonoids (hesperetin and cianidanol) displayed moderate RMSF values (~1.05–1.09 Å), aligning with their favorable pharmacokinetic profiles [52]. Cianidanol, despite having the weakest docking affinity (−6.8 kcal/mol), exhibited stable RMSF distribution with high hydrogen-bonding interactions, suggesting that it maintains consistent engagement with MAPK1 over the simulation trajectory. These findings reinforce that *M. oleifera* compounds engage MAPK1 in a stable and dynamically favorable manner, complementing earlier docking results. The sterol compounds achieve strong affinity with moderate flexibility, while flavonoids offer stable, pharmacokinetically favorable binding. While these findings provide strong mechanistic hypotheses for MAPK1–STAT3 modulation by *M. oleifera*, they remain predictive in nature and do not constitute direct evidence of therapeutic efficacy. This duality underscores the polypharmacological nature of *M. oleifera* in AD therapy: sterols may serve as potent but less bioavailable scaffolds for MAPK1 inhibition, whereas flavonoids represent safer, more suitable nutraceutical leads.

5. Conclusion

This study demonstrates that *M. oleifera* harbors multiple bioactive compounds with significant therapeutic potential against AD through a network of multi-target interactions. Key hub proteins such as MAPK1, STAT3, and HSP90AA1 emerged as critical mediators of its effects, particularly in pathways governing synaptic function, neuroinflammation, and amyloid-beta toxicity. Molecular docking highlighted strong affinities of sterol-based compounds with MAPK1, while ADMET profiling indicated hesperetin and cianidanol as promising, safer leads. *M. oleifera* represents a valuable source of multi-target neuroprotective agents. These results represent an in silico prediction framework that prioritizes MAPK1 and STAT3 as candidate targets for *M. oleifera* phytochemicals, warranting future experimental validation. This work provides a mechanistic foundation for future experimental validation, structural optimization, and possible nutraceutical or therapeutic development targeting AD.

6. Limitations

Target prediction and docking rely on in silico algorithms that may not fully capture biological complexity or in vivo pharmacokinetics. No in vitro or in vivo assays were performed to confirm predicted interactions or pharmacological efficacy. ADMET and ProTox results are predictive and require experimental toxicological validation. A limitation of this study is the absence of extended MD simulations (e.g., RMSD, radius of gyration, hydrogen bond stability, and free energy calculations using GROMACS). Such analyses would provide deeper insights into the long-term stability and conformational dynamics of protein–ligand complexes. However, due to resource constraints at the undergraduate research level, we employed CABS-flex 2.0 simulations, which offer a coarse-grained yet efficient approximation of protein flexibility. Target prediction databases rely on chemical similarity and known ligand–target associations, which may bias predictions toward well-characterized proteins. Likewise, docking scores are approximations of binding affinity and do not account for full protein flexibility or cellular context. Future work incorporating full atomistic MD simulations on high-performance computing platforms is strongly recommended.

Ethical Statement

This study did not involve any experiments on human participants or animal subjects. All analyses were conducted using data retrieved from publicly available databases, including phytochemical repositories, disease-gene databases, and protein structure databases. These data were generated and shared in accordance with the ethical standards and approvals reported in the respective original sources. Therefore, no additional ethical approval or informed consent was required for the present study.

Conflicts of Interest

The authors declare that they have no conflicts of interest to this work. The authors declare that there are no known competing financial interests or personal relationships that could have appeared to influence the work reported in this paper.

Data Availability Statement

The present study did not generate any new experimental data. All data used in this work were retrieved from publicly available databases, including phytochemical databases (such as PubChem), disease-associated gene databases, and protein structure repositories (Protein Data Bank). These resources are publicly accessible, and all relevant database sources are appropriately cited within the manuscript.

Author Contribution Statement

Israr Hussain: Methodology, Writing – original draft. **Itazaz Ul Haq:** Methodology. **Muhammad Rahiyab:** Software. **Li Pinyi:** Validation, Data curation. **Ishaq Khan:** Resources. **Syed Shujait Ali:** Writing – review & editing, Visualization. **Mohammad Ali:** Investigation. **Arshad Iqbal:** Conceptualization, Formal analysis, Supervision, Project administration.

References

[1] Scheltens, P., De Strooper, B., Kivipelto, M., Holstege, H., Chételat, G., Teunissen, C. E., . . . , & van der Flier, W. M. (2021). Alzheimer's disease. *The Lancet*, *397*(10284), 1577–1590. https://doi.org/10.1016/S0140-6736(20)32205-4

[2] Song, C., Shi, J., Zhang, P., Zhang, Y., Xu, J., Zhao, L., . . . , & Chen, H. (2022). Immunotherapy for Alzheimer's disease: Targeting β-amyloid and beyond. *Translational Neurodegeneration*, *11*(1), 18. https://doi.org/10.1186/s40035-022-00292-3

[3] Goel, F. (2025). Exploring the therapeutic role of Moringa oleifera in neurodegeneration: Antioxidant, anti-inflammatory, and neuroprotective mechanisms: Exploring the therapeutic role of Moringa oleifera in neurodegeneration. *Inflammopharmacology*, *33*, 3653–3669. https://doi.org/10.1007/s10787-025-01794-y

[4] Chhikara, N., Kaur, A., Mann, S., Garg, M. K., Sofi, S. A., & Panghal, A. (2021). Bioactive compounds, associated health benefits and safety considerations of Moringa oleifera L.: An updated review. *Nutrition & Food Science*, *51*(2), 255–277. https://doi.org/10.1108/NFS-03-2020-0087

[5] Saleh, A. Y., Saputra, D. A. Y., Valentina, R., & Susanto, T. D. (2025). The miracle Moringa oleifera tree: A bibliometric review of its neuroprotective properties. *Pharmacognosy Journal*, *17*(2), 258–276. http://doi.org/10.5530/pj.2025.17.33

[6] Aljadaan, A. M., AlSaadi, A. M., Shaikh, I. A., Whitby, A., Ray, A., Kim, D. H., & Carter, W. G. (2025). Characterization of the anticholinesterase and antioxidant properties of phytochemicals from Moringa oleifera as a potential treatment for Alzheimer's disease. *Biomedicines*, *13*(9), 2148. https://doi.org/10.3390/biomedicines13092148

[7] Qasim, M., Abdullah, M., Ashfaq, U. A., Noor, F., Nahid, N., Alzamami, A., . . . , & Khurshid, M. (2023). Molecular mechanism of Ferula asafoetida for the treatment of asthma: Network pharmacology and molecular docking approach. *Saudi Journal of Biological Sciences*, *30*(2), 103527. https://doi.org/10.1016/j.sjbs.2022.103527

[8] Paul, A., Zothantluanga, J. H., Rakshit, G., Celik, I., Rudrapal, M., & Zaman, M. K. (2024). Computational simulations reveal the synergistic action of phytochemicals of Morus alba to exert anti-Alzheimer activity via inhibition of acetylcholinesterase and glycogen synthase kinase-3β. *Polycyclic Aromatic Compounds*, *44*(5), 3476–3500. https://doi.org/10.1080/10406638.2023.2236759

[9] Yang, L., Wang, H., Zhu, Z., Yang, Y., Xiong, Y., Cui, X., & Liu, Y. (2025). Network pharmacology-driven sustainability: AI and multi-omics synergy for drug discovery in traditional Chinese medicine. *Pharmaceuticals*, *18*(7), 1074. https://doi.org/10.3390/ph18071074

[10] Narykov, O., Zhu, Y., Brettin, T., Evrard, Y. A., Partin, A., Shukla, M., . . . , & Stevens, R. L. (2023). Integration of computational docking into anti-cancer drug response prediction models. *Cancers*, *16*(1), 50. https://doi.org/10.3390/cancers16010050

[11] Vivek-Ananth, R. P., Mohanraj, K., Sahoo, A. K., & Samal, A. (2023). IMPPAT 2.0: An enhanced and expanded phytochemical atlas of Indian medicinal plants. *ACS Omega*, *8*(9), 8827–8845. https://doi.org/10.1021/acsomega.3c00156

[12] Abdel-Maksoud, M. A., Askar, M. A., Abdel-Rahman, I. Y., Gharib, M., & Aufy, M. (2024). Integrating network pharmacology and molecular docking approach to elucidate the mechanism of Commiphora wightii for the treatment of rheumatoid arthritis. *Bioinformatics and Biology Insights*, *18*, 11779322241247634. https://doi.org/10.1177/11779322241247634

[13] White, J. (2020). PubMed 2.0. *Medical Reference Services Quarterly*, *39*(4), 382–387. https://doi.org/10.1080/02763869.2020.1826228

[14] Martín-Martín, A., Thelwall, M., Orduna-Malea, E., & Delgado López-Cózar, E. (2021). Google Scholar, Microsoft Academic, Scopus, Dimensions, Web of Science, and OpenCitations' COCI: A multidisciplinary comparison of coverage via citations. *Scientometrics*, *126*(1), 871–906. https://doi.org/10.1007/s11192-020-03690-4

[15] Riyadi, P. H., Romadhon, Sari., D, I., Kurniasih, R. A., Agustini, T. W., Swastawati, F., . . . , & Tanod, W. A. (2021). SwissADME predictions of pharmacokinetics and drug-likeness properties of small molecules present in Spirulina platensis. *In IOP Conference Series: Earth and Environmental Science*, *890*(1), 012021. https://doi.org/10.1088/1755-1315/890/1/012021

[16] Ononamadu, C. J., & Ibrahim, A. (2021). Molecular docking and prediction of ADME/drug-likeness properties of potentially active antidiabetic compounds isolated from aqueous-methanol extracts of Gymnema sylvestre and Combretum micranthum. *BioTechnologia*, *102*(1), 85. https://doi.org/10.5114/bta.2021.103765

[17] Kim, S., Chen, J., Cheng, T., Gindulyte, A., He, J., He, S., . . . , & Bolton, E. E. (2023). PubChem 2023 update. *Nucleic Acids Research*, *51*(D1), D1373–D1380. https://doi.org/10.1093/nar/gkac956

[18] Ghani, S. S. (2020). A comprehensive review of database resources in chemistry. *Eclética Química*, *45*(3), 57–68. https://doi.org/10.26850/1678-4618eqj.v45.3.2020.p57-68

[19] Ji, K. Y., Liu, C., Liu, Z. Q., Deng, Y. F., Hou, T. J., & Cao, D. S. (2023). Comprehensive assessment of nine target prediction web services: Which should we choose for target fishing? *Briefings in Bioinformatics*, *24*(2), bbad014. https://doi.org/10.1093/bib/bbad014

[20] Wang, H., Li, Y., Liu, X., & Wu, Y. (2024). Identification and validation of ferroptosis-related gene SLC2A1 as a novel prognostic biomarker in AKI. *Aging (Albany, NY)*, *16*(6), 5634. https://doi.org/10.18632/aging.205669

[21] Movazeb, E., Flores, C., Ríos, R., Ríos, S., Fu, L., & Mendez-Rios, J. D. (2025). Evaluación y clasificación de artículos relacionados al gen MTHFR y evidencia OMIM. *Genetics and Clinical Genomics*, *3*(1), 2599. https://doi.org/10.37980/im.journal.ggcl.en.20252599

[22] Ahmad, S., Jose da Costa Gonzales, L., Bowler-Barnett, E. H., Rice, D. L., Kim, M., Wijerathne, S., . . . , & Martin, M. J. (2025). The UniProt website API: Facilitating programmatic access to protein knowledge. *Nucleic Acids Research*, *53*(W1), W547–W553. https://doi.org/10.1093/nar/gkaf394

[23] Zhou, C., Zhou, Z. M., Hu, L., Yang, Y. Y., Meng, X. W., & Yang, X. S. (2021). Identification and verification of the effect of miR-143 on the cardioprotective role of phosphocreatine in doxorubicin-induced cardiotoxicity by integrated bioinformatics analysis. https://doi.org/10.21203/rs.3.rs-1168472/v1

[24] Szklarczyk, D., Nastou, K., Koutrouli, M., Kirsch, R., Mehryary, F., Hachilif, R., . . . , & von Mering, C. (2025). The STRING database in 2025: Protein networks with directionality of regulation. *Nucleic Acids Research*, *53*(D1), D730–D737. https://doi.org/10.1093/nar/gkae1113

[25] Bathla, D., & Vindal, V. (2026). Protein interaction network analysis: STRING and CYTOSCAPE. In L. N. R. Vemireddy, B. Reddyyamini, & Y. Amaravathi (Eds.), *Harnessing genomic tools for crop improvement* (pp. 393–418). Academic Press. https://doi.org/10.1016/B978-0-443-29281-1.00006-X

[26] Sherman, B. T., Hao, M., Qiu, J., Jiao, X., Baseler, M. W., Lane, H. C., . . . , & Chang, W. (2022). DAVID: A web server for functional enrichment analysis and functional annotation of gene lists (2021 update). *Nucleic Acids Research*, *50*(W1), W216–W221. https://doi.org/10.1093/nar/gkac194

[27] Tang, D., Chen, M., Huang, X., Zhang, G., Zeng, L., Zhang, G., . . . , & Wang, Y. (2023). SRplot: A free online platform for data visualization and graphing. *PloS One*, *18*(11), e0294236. https://doi.org/10.1371/journal.pone.0294236

[28] Burley, S. K., Bhikadiya, C., Bi, C., Bittrich, S., Chao, H., Chen, L., . . . , & Zardecki, C. (2023). RCSB Protein Data Bank (RCSB. org): Delivery of experimentally-determined PDB structures alongside one million computed structure models of proteins from artificial intelligence/machine learning. *Nucleic Acids Research*, *51*(D1), D488–D508. https://doi.org/10.1093/nar/gkac1077

[29] Shelton, V. (2025). Determining the effectivity of PyMOL approaches through the experimental evaluation of lactoferrin binding. *Cambridge Open Engage*. https://doi.org/10.33774/coe-2025-0qpwr

[30] Kondapuram, S. K., Sarvagalla, S., & Coumar, M. S. (2021). Docking-based virtual screening using PyRx Tool: Autophagy target Vps34 as a case study. In M. S. Coumar (Ed.), *Molecular docking for computer-aided drug design* (pp. 463–477). Academic Press. https://doi.org/10.1016/B978-0-12-822312-3.00019-9

[31] Mane, P. T., Wakure, B. S., & Wakte, P. S. (2022). Binary and ternary inclusion complexation of lapatinib ditosylate with β-cyclodextrin: Preparation, evaluation and in vitro anticancer activity. *Beni-Suef University Journal of Basic and Applied Sciences*, *11*(1), 150. https://doi.org/10.1186/s43088-022-00332-x

[32] Sharma, S., Sharma, A., & Gupta, U. (2021). Molecular docking studies on the anti-fungal activity of *Allium sativum* (garlic) against mucormycosis (black fungus) by BIOVIA discovery studio visualizer 21.1.0.0. https://doi.org/10.21203/rs.3.rs-888192/v1

[33] Khare, S., Chatterjee, T., Gupta, S., & Ashish, P. (2023). Bioavailability predictions, pharmacokinetics and drug-likeness of bioactive compounds from Andrographis paniculata using Swiss ADME. *MGM Journal of Medical Sciences*, *10*(4), 651–659. https://doi.org/10.4103/mgmj.mgmj_245_23

[34] Banerjee, P., Kemmler, E., Dunkel, M., & Preissner, R. (2024). ProTox 3.0: A webserver for the prediction of toxicity of chemicals. *Nucleic Acids Research*, *52*(W1), W513–W520. https://doi.org/10.1093/nar/gkae303

[35] Wróblewski, K., Zalewski, M., Kuriata, A., & Kmiecik, S. (2025). CABS-flex 3.0: An online tool for simulating protein structural flexibility and peptide modeling. *Nucleic Acids Research*, *53*(W1), W95–W101. https://doi.org/10.1093/nar/gkaf412

[36] Biswas, P., Adhikari, A., Pal, U., Singh, P., Das, M., Saha-Dasgupta, T., . . . , & Pal, S. K. (2020). Flexibility modulates the catalytic activity of a thermostable enzyme: Key information from optical spectroscopy and molecular dynamics simulation. *Soft Matter*, *16*(12), 3050–3062. https://doi.org/10.1039/C9SM02479D

[37] Detka, J., Płachtij, N., Strzelec, M., Manik, A., & Sałat, K. (2024). p38α mitogen-activated protein kinase—an emerging drug target for the treatment of Alzheimer's disease. *Molecules*, *29*(18), 4354. https://doi.org/10.3390/molecules29184354

[38] Gee, M. S., Son, S. H., Jeon, S. H., Do, J., Kim, N., Ju, Y. J., . . . , & Lee, J. K. (2020). A selective p38α/β MAPK inhibitor alleviates neuropathology and cognitive impairment, and modulates microglia function in 5XFAD mouse. *Alzheimer's Research & Therapy*, *12*(1), 45. https://doi.org/10.1186/s13195-020-00617-2

[39] Hossain, R., Noonong, K., Nuinoon, M., Majima, H. J., Eawsakul, K., Sompol, P., . . . , & Tangpong, J. (2024). Network pharmacology, molecular docking, and in vitro insights into the potential of Mitragyna speciosa for Alzheimer's disease. *International Journal of Molecular Sciences*, *25*(23), 13201. https://doi.org/10.3390/ijms252313201

[40] Sharifi-Rad, J., Rapposelli, S., Sestito, S., Herrera-Bravo, J., Arancibia-Diaz, A., Salazar, L. A., . . . , & Calina, D. (2022). Multi-target mechanisms of phytochemicals in Alzheimer's disease: Effects on oxidative stress, neuroinflammation and protein aggregation. *Journal of Personalized Medicine*, *12*(9), 1515. https://doi.org/10.3390/jpm12091515

[41] Deng, Y., Zhang, J., Sun, X., Ma, G., Luo, G., Miao, Z., & Song, L. (2020). miR-132 improves the cognitive function of rats with Alzheimer's disease by inhibiting the MAPK1 signal pathway. *Experimental and Therapeutic Medicine*, *20*(6), 159. https://doi.org/10.3892/etm.2020.9288

[42] Patwekar, M., Patwekar, F., Shaikh, D., Fatema, S. R., Aher, S. J., & Sharma, R. (2023). Receptor-based approaches and therapeutic targets in Alzheimer's disease along with role of AI in drug designing: Unraveling pathologies and advancing treatment strategies. *Applied Chemical Engineering*, *6*(3). https://doi.org/10.24294/ace.v6i3.2338

[43] Woods, N. K., & Padmanabhan, J. (2012). Neuronal calcium signaling and Alzheimer's disease. In M. Islam (Ed.), *Calcium signaling* (*vol 740*, (1193-1217). Springer. https://doi.org/10.1007/978-94-007-2888-2_54

[44] Huang, S., Zhang, Y., Shu, H., Liu, W., Zhou, X., & Zhou, X. (2024). Advances of the MAPK pathway in the treatment of spinal cord injury. *CNS Neuroscience & Therapeutics*, *30*(6), e14807. https://doi.org/10.1111/cns.14807

[45] Dhapola, R., Beura, S. K., Sharma, P., Singh, S. K., & HariKrishnaReddy, D. (2024). Oxidative stress in Alzheimer's disease: Current knowledge of signaling pathways and therapeutics. *Molecular Biology Reports*, *51*(1), 48. https://doi.org/10.1007/s11033-023-09021-z

[46] Lee, E., Song, C. H., Bae, S. J., Ha, K. T., & Karki, R. (2023). Regulated cell death pathways and their roles in homeostasis, infection, inflammation, and tumorigenesis. *Experimental & Molecular Medicine*, *55*(8), 1632–1643. https://doi.org/10.1038/s12276-023-01069-y

[47] Jain, M., Singh, M. K., Shyam, H., Mishra, A., Kumar, S., Kumar, A., & Kushwaha, J. (2021). Role of JAK/STAT in the neuroinflammation and its association with neurological disorders. *Annals of Neurosciences*, *28*(3-4), 191–200. https://doi.org/10.1177/09727531211070532

[48] Sharma, A., Mehra, V., Kumar, V., & Prakash, H. (2023). Tailoring MAPK pathways: New therapeutics avenues for managing Alzheimer's diseases. *Preprints*. https://doi.org/10.20944/preprints202312.1509.v1

[49] Cummings, J. L., Teunissen, C. E., Fiske, B. K., Le Ber, I., Wildsmith, K. R., Schöll, M., . . . , & Scheltens, P. (2025). Biomarker-guided decision making in clinical drug development for neurodegenerative disorders. *Nature Reviews Drug Discovery*, *24*, 589–609. https://doi.org/10.1038/s41573-025-01165-w

[50] Rao, C. M. P., Silakabattini, K., Narapusetty, N., Marabathuni, V. J. P., Thejomoorthy, K., Rajeswari, T., & Sabitha, Y. (2023). Insights from the molecular docking and simulation analysis of P38 MAPK phytochemical inhibitor complexes. *Bioinformation*, *19*(3), 323–330. https://doi.org/10.6026/97320630019323

[51] Hollingsworth, S. A., Kelly, B., Valant, C., Michaelis, J. A., Mastromihalis, O., Thompson, G., . . . , & Dror, R. O. (2019). Cryptic pocket formation underlies allosteric modulator selectivity at muscarinic GPCRs. *Nature Communications*, *10*(1), 3289. https://doi.org/10.1038/s41467-019-11062-7

[52] Hang, L., Hu, F., Shen, C., Shen, B., Zhu, W., & Yuan, H. (2021). Development of herpetrione nanosuspensions stabilized by glycyrrhizin for enhancing bioavailability and synergistic hepatoprotective effect. *Drug Development and Industrial Pharmacy*, *47*(10), 1664–1673. https://doi.org/10.1080/03639045.2022.2045304

How to Cite: Hussain, I., Haq, I. U., Rahiyab, M., Pinyi, L., Khan, I., Ali, S. S., …, & Iqbal, A. (2026). Integrative Network Pharmacology and Docking Analysis of *Moringa oleifera* in Alzheimer's Disease: Dual Targeting of MAPK1 and STAT3 by Active Phytochemical Compounds. *Medinformatics*. https://doi.org/10.47852/bonviewMEDIN62028824